

1
2
3
4 **Calibration of low-cost particulate matter sensors for coal dust monitoring**
5
67 Nana A. Amoah^a
8
910 a. Department of Mining and Explosives Engineering, Missouri University of Science and
11 Technology, 1870 Miner Circle, Rolla, Missouri, 65401, USA
12
1314 Guang Xu^{a*}
15
1617 a. Department of Mining Engineering, Missouri University of Science and Technology,
18 1870 Miner Circle, Rolla, Missouri, 65401, USA
19
20 Ashish Kumar^b
21
22 b. Department of Energy and Mineral Engineering, Pennsylvania State University, 201 Old
23 Main, University Park, Pennsylvania 16802, USA
24
25 Yang Wang^c
26
2728 c. Department of Chemical, Environmental and Materials Engineering, University of
29 Miami, 1320 S Dixie Hwy, Coral Gables, Florida 33124, USA
30
31
32
33
34
35
36
3738 *To whom correspondence should be addressed:
39
40
41 Address: 1400 N Bishop Ave 288., Rolla, Mo., USA
42
43 Tel: +1-573-202-8919
44
45
46 Email: guang.xu@mst.edu
47
48
49
50
51
52
53
54
55
56
57
58
59
60
61
62
63
64
65

1 **Calibration of low-cost particulate matter sensors for coal dust monitoring**

2 **Abstract**

3 Mining-induced coal dust causes various respiratory diseases to mine workers mainly coal
4 workers' pneumoconiosis (CWP). Currently available underground monitors are expensive and
5 bulky. These disadvantages limit them for regulatory sample monitoring purposes. Moreover,
6 personal exposure levels for most miners remain unknown, risking them to potential overexposures.
7 Low-cost light scattering particulate matter (PM) sensors offer a potential solution to this problem
8 with the capability to characterize PM concentration with high spatio-temporal resolution.
9 However, these sensors require precise calibration before they can be deployed in mining
10 environments. No previous study has promulgated a standard protocol to assess these sensors for
11 coal dust monitoring. The goal of this study was to calibrate Plantower PMS5003 sensors for coal
12 dust monitoring using linear regression models. Two other commercially available PM sensors,
13 the Airtrek and Gaslab CM-505 multi-gas sensors, were also evaluated and calibrated. They were
14 evaluated for factors including linearity, precision, limit of detection, upper concentration limits,
15 and the influence of temperature and relative humidity in a laboratory wind tunnel. The PMS5003
16 sensors were observed to be accurate below 3.0 mg/m^3 concentration levels with R-squared values
17 of 0.70 to 0.90 which was the best among the sensors under with an acceptable precision below
18 1.5 mg/m^3 . Moreover, this study shows that temperature and relative humidity have minimal
19 influence on the efficacy of low-cost PM sensors' ability to monitor coal dust. This investigation
20 reveals the feasibility of low-cost sensors for real-time personal coal dust monitoring in
21 underground coal mines if a robust calibration model is applied.

22

23 **1 Introduction**

24 Coal dust concentrations in underground mines can be considerably higher than surface mines
25 due to limited ventilation to dilute the coal dust. This puts underground mine workers at a greater
26 risk of coal dust overexposure. Overexposure to respirable coal mine dust (RCMD) has resulted in
27 the onset of irreversible diseases, such as coal workers' pneumoconiosis (CWP), emphysema and
28 chronic bronchitis collectively known as 'black lung' which can cause permanent disability and
29 premature death (MSHA, 2014). Miners have also been diagnosed with silicosis due to exposure

30 to coal dust with high silica contents (Knight et al., 2020; D. Wang et al., 2020). In recent times,
31 there has been a resurgence of CWP among US coal miners (Blackley et al., 2016) which is of
32 great concern to the mining industry. Contrary to common understanding that CWP is only
33 associated with long-term coal dust exposure, recent data indicates that advanced CWP has been
34 found in younger coal miners (MSHA, 2014).

35 Accurate real-time personal dust exposure monitoring is essential to alert mine workers to
36 change behavior and apply mitigation methods to reduce their exposure when working. The Mine
37 Safety and Health Administration (MSHA) requires the use of continuous personal dust monitors
38 (CPDM) for measuring RCMD mass concentrations and determining compliance with the
39 regulatory exposure limits. However, current CPDM devices are expensive and bulky (Badura et
40 al., 2018; Barakeh et al., 2017; Kelleher et al., 2018; P. Kumar et al., 2015). For example,
41 PDM3700 is the MSHA certified CPDM to be used in coal mines, but it costs ~\$17,000 and weighs
42 2.0 kg (Haltermann et al., 2018). These expensive PDMs are worn only by a few miners for
43 regulatory compliance monitoring. These are mainly miners who are exposed to the highest coal
44 dust concentrations at their work locations and those who have already been diagnosed with
45 pneumoconiosis (MSHA, 2014). This practice has serious drawbacks, most notably is that the
46 exposure levels for most miners are unknown. Besides, dust control effectiveness of modified
47 engineering control strategies is not well understood by mining engineers due to lack of sufficient
48 monitoring data. Finally, there is a lack of sufficient exposure information to accurately correlate
49 coal dust exposure to its related-health data in epidemiology studies.

50 Light scattering low-cost particulate matter (PM) sensors have the potential to accurately
51 monitor coal dust concentration in real time. The low cost, small size, and low power requirements
52 of these sensors offer the promise of being widely worn by all coal mine workers. These could
53 yield accurate concentration information if properly calibrated. Even though this technology has
54 been significantly explored by researchers for other environmental applications (Kelly et al., 2017;
55 Li, 2019; Sousan et al., 2016; Y. Wang, Li, Jing, Zhang, Jiang, & Biswas, 2015a), it remains a new
56 technology for monitoring coal dust (Amoah et al., 2022). Because of questionable accuracy and
57 long-term reliability of these sensors, it is critical to adopt a systematic approach to evaluate and
58 effectively calibrate these sensors before they can be applied for coal dust monitoring. Many low-cost
59 PM sensor calibration studies have demonstrated promising results in comparison with

60 Federal Equivalent Methods (FEMs) or research-grade instruments for air quality PM monitoring
61 (Chen et al., 2019; De Vito et al., 2008; D. Liu et al., 2017; Spinelle et al., 2013; Y. Wang, Li, Jing,
62 Zhang, Jiang, & Biswas, 2015b). However, there are very few studies that investigate the
63 performance and application of low-cost sensors for monitoring coal dust. Existing research by
64 governmental agencies such as US Environmental Protection Agency (EPA) (Williams et al., 2014)
65 and European Metrology Research Program (EURAMET) (Spinelle et al., 2013), as well as
66 research in the literature (Y. Wang, Li, Jing, Zhang, Jiang, & Biswas, 2015a) have established
67 standard protocols for calibrating low-cost PM sensors for environmental PM monitoring.
68 However, there is still limited understanding of how these calibration models will perform with
69 mining-induced coal dust.

70 The objective of this study was to evaluate and calibrate three types of lower cost PM sensors
71 against a FEM reference monitor, Personal Dust Monitor (PDM) model 3700 and a research grade
72 Aerodynamic Particle Sizer (APS) model 3321. A custom-built wind tunnel in the laboratory was
73 used for the calibration experiments. Sensors and monitors were exposed to various levels of
74 concentration within the tunnel to generate the linearity plots between the sensors and the reference
75 monitors. Since several studies have established the linear relationship between light scattering
76 low-cost PM sensors and reference monitors, univariate calibration models using linear regression
77 were developed based on the linearity analysis to calibrate the sensors (Austin et al., 2015;
78 Ghamari et al., 2022; Kelly et al., 2017; Liu et al., 2017; Polidori et al., 2016). The precision, limit
79 of detection and upper concentration limits were evaluated to provide further understanding of the
80 sensors' performance with coal dust. A 2^2 factorial design was used to determine the influence of
81 temperature and relative humidity (RH) on the sensors' performance at low ($\sim 0.5 \text{ mg/m}^3$) and high
82 ($\sim 1.5 \text{ mg/m}^3$) coal dust concentration levels. This method provides an understanding of the
83 influence of each of the two levels of both temperature and RH on sensor outputs as well as the
84 interaction of both conditions. The implementation of these sensors for coal dust monitoring will
85 expand personal exposure monitoring in mines as every miner can wear one to detect timely
86 overexposures to ensure timely controls are engineered to protect miners' health. On a broader
87 scope, low-cost PM sensors can greatly supplement more expensive research grade monitors used
88 in other occupational environments.

89 2 Experimental Methods

90 2.1 Low-Cost PM sensors and reference monitors

91 Three low-cost PM sensors were evaluated in this study – the Plantower PMS50003 (PMS)
92 low-cost PM sensor, the Airtrek PM sensor, and the Gaslab CM-505 multi-gas sensor. Two units
93 of each sensor were evaluated. The Gaslab sensor, shown in Figure 1 (a) measures PM 2.5 and PM
94 10 particle concentration together with oxygen, carbon dioxide and carbon monoxide
95 concentrations. The Gaslab uses a combination of NDIR sensors, electrochemical sensors, and
96 fluorescent sensors to measure gases and uses laser scattering technology to measure PM 2.5 and
97 PM 10. The Airtrek sensors on the other hand, shown in Figure 1 (b) use light scattering principles
98 like that of the Plantower PMS5003 sensor to measure PM concentrations. The Airtrek sensors
99 measure PM in four size bins of 1.0 μm , 2.5 μm , 4.0 μm , and 10.0 μm .

100 The Plantower PMS5003 (shown in Figure 1(d)) was used to assemble in-house made dust
101 monitors. They are inexpensive light scattering PM sensors that are commercially available for
102 about \$ 30. This sensor employs a fan to draw ambient air into the light scattering measuring cavity
103 through its inlet. As illustrated in Figure 1 (c), the LED radiates laser-induced light into the sensing
104 area to target particles within the measuring cavity. Light is scattered as it hits the particles. It is
105 detected by the photo-diode detector, which is positioned at 180° with the LED light. The scattered
106 light received by the photo-diode detector sends pulses of electric signal to the in-built
107 microprocessor. The number and intensity of electrical signals detected by the microprocessor are
108 then converted to number and mass of particles respectively based on MIE theory (Yong & Haoxin,
109 2016).

110 These PMS sensors characterize PM by size into PM1, PM2.5, and PM10. The manufacturers
111 of the PMS sensors state that PM1 is measured for particles in the size range of 0.3 μm to 1.0 μm ,
112 PM2.5 for particles in the size range of 1.0 μm to 2.5 μm and PM10 for particles in the size range
113 of 2.5 μm to 10.0 μm . For each size category, the PMS reports two PM outputs, one without any
114 form of correction factor, called standard PM concentration (or CF = 1) and the other with an
115 atmospheric calibration factor, called environmental PM concentration. The manufacturers have
116 not published any details about the calibration factor and how it was developed. Therefore, due to
117 considerable uncertainties about manufacturer calibration, the standard PM concentrations were

118 used for this study. Manufacturer specifications indicated high anti-interference performance using
119 non-PM shielding technology. Previous studies have also shown that the Plantower sensors have
120 superior performance as they have been integrated into PurpleAir air quality monitors (Sayahi et
121 al., 2019). These characteristics justify the reason the PMS sensors were used for this study.

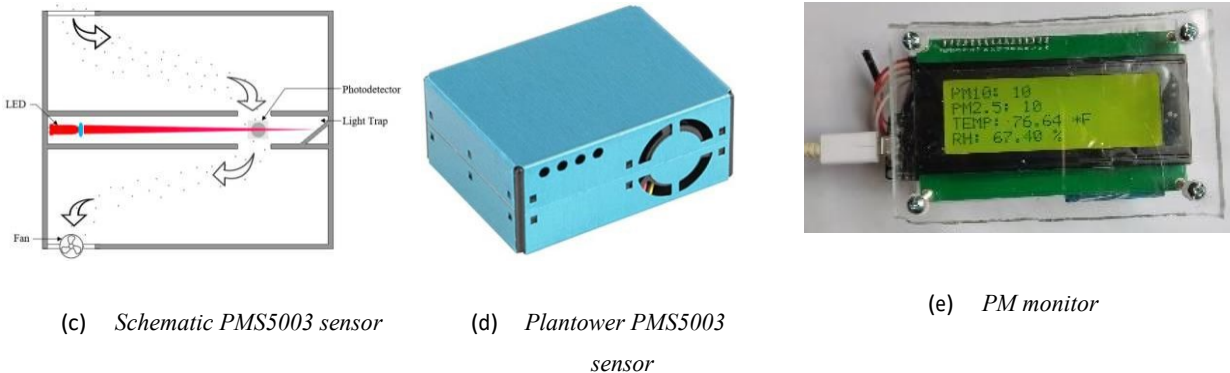
122 Together with a DHT-22 temperature and relative humidity sensor, NodeMCU ESP8266
123 (Systems, 2015) and a 4 line by 20-character LCD screen, the PMS5003 was integrated into a
124 prototype monitor (low-cost PM monitor) as displayed in Figure 1 (e). This monitor was
125 programmed with Arduino IDE to display real time concentrations of PM2.5 and PM10,
126 temperature and relative humidity readings every 1.0 s onto the LCD screen. To protect the low-127
cost PM sensor and its critical components from rainfall, sunlight, and physical damage, the sensor,
128 and its components are housed in a 10.0 cm x 4.0 cm x 1.5 cm acrylic plastic box. This also allowed 129
the team to see the screen readings in real time through the transparent acrylic case. The side of 130
the acrylic case is strongly fastened but left uncovered to allow for normal operation of the PMS 131
sensor without interference to the sensors' exposure. The low-cost PM monitor is continuously 132
powered using a 5.0 V USB cable. For data analysis, the PM monitor is interfaced with a 133
ThingSpeak Matlab based online IOT platform which serves as a cloud where all data is 134
transmitted through Wi-Fi.



(a) Gaslab CM-505 multi-gas sensor



(b) Airtrek PM sensor



136 *Figure 1. Low-cost PM monitor: (a) schematic diagram of the plantower PMS5003, (b) a picture of the Plantower*
 137 *PMS5003 sensor; (c) the in house fabricated low-cost PM monitor*

138 The primary reference monitor used in this study is the personal dust monitor model 3700
 139 (PDM3700). This is a real time personal coal dust monitor which operates on the principle of
 140 tapered element oscillation microbalance (TEOM). It is capable of reporting concentrations at 1-
 141 minute intervals. The PDM3700 is equipped with a respirable size inlet installed near the inlet
 142 which ensures that the cut-off diameter for coal dust going through the mass sensor is $5.0 \mu\text{m}$. This
 143 makes it capable of monitoring respirable size coal particles. It is used by miners by mounting the
 144 sample inlet, incorporated in the universal cap lamp, on the bill of a miner's hard hat to monitor
 145 dust within the miner's breathing zone (Volkwein et al., 2006). The National Institute for
 146 Occupational Safety and Health (NIOSH) has validated PDM3700's accuracy, precision, and
 147 comfortability, and Mine Safety and Health Administration (MSHA) has approved this equipment
 148 as the regulatory compliance monitoring device (Volkwein et al., 2006). This has also been
 149 designated as Federal Equivalent Method by the U.S. Environmental Protection Agency (EPA) for
 150 environmental air quality PM monitoring (US-EPA, 2012).

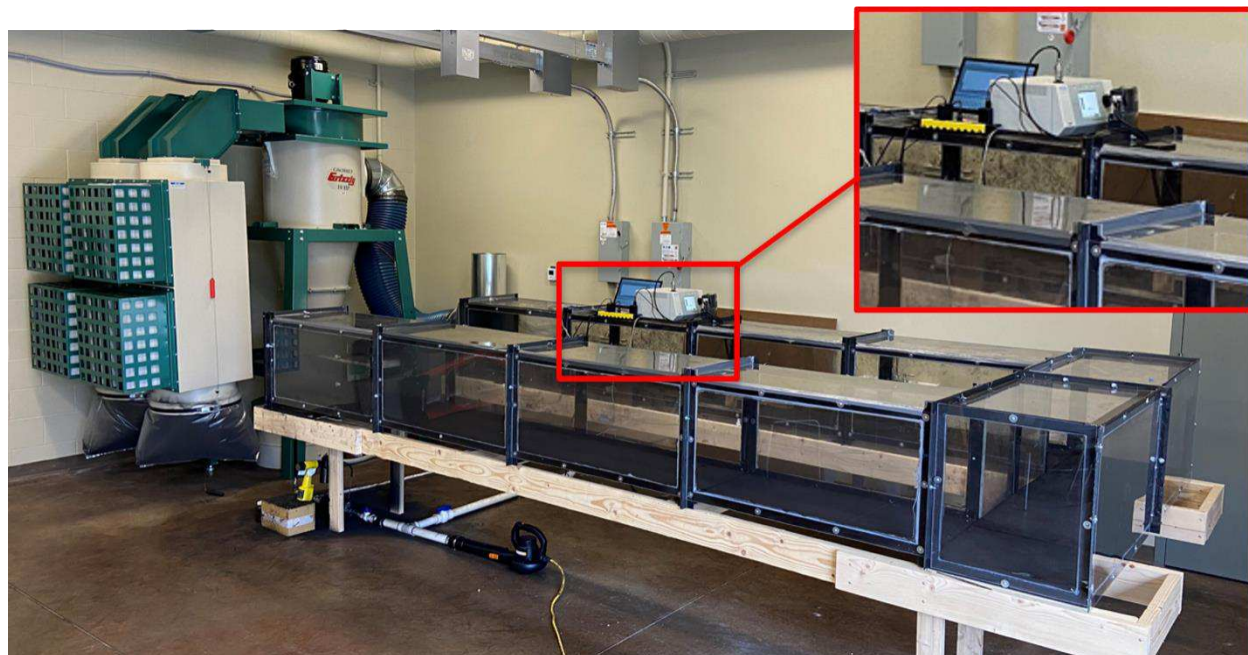
151 The APS measures PM mass and number concentration by particle aerodynamic sizes from $0.5 \mu\text{m}$ to $20.0 \mu\text{m}$ using the time-of-flight principles. To make it comparable with the PDM, PM
 152 concentration of particle size ranging from 0.00 to $4.37 \mu\text{m}$ from the APS was used for this study
 153 since it compares with the $4.37 \mu\text{m}$ D_{50} of the PDM cyclone. The APS draws ambient PM-laden
 154 air into the monitor through a nozzle at an accelerated flowrate of 5.0 liters per minute. Ideally, the
 155 APS needs to sample airflow at the same velocity as the air velocity at the sampling location. In
 156 this case, a 0.8 cm diameter nozzle was used to achieve a sampling velocity of 1.5 m/s to get as
 157 close as possible to airflow velocity in the wind tunnel. The accelerated airflow goes through the
 158

159 sensing zone where the PM concentrations are measured using the time-of-flight principles.
160 Particle size distribution is then reported every 15 seconds based on the settings used for this study
161 (TSI Inc., 2017).

162 **2.2 Wind tunnel**

163 The calibration chamber used in this study is a custom-built wind tunnel made with metal
164 frames and acrylic glass panels (Figure 2). The wind tunnel has a U shape with cross-sectional
165 dimension of the tunnel being 0.5 m x 0.5 m to simulate the airway bends in underground mines.
166 The entire dimension of the U shape is 4.5 m long and 2.0 m wide.

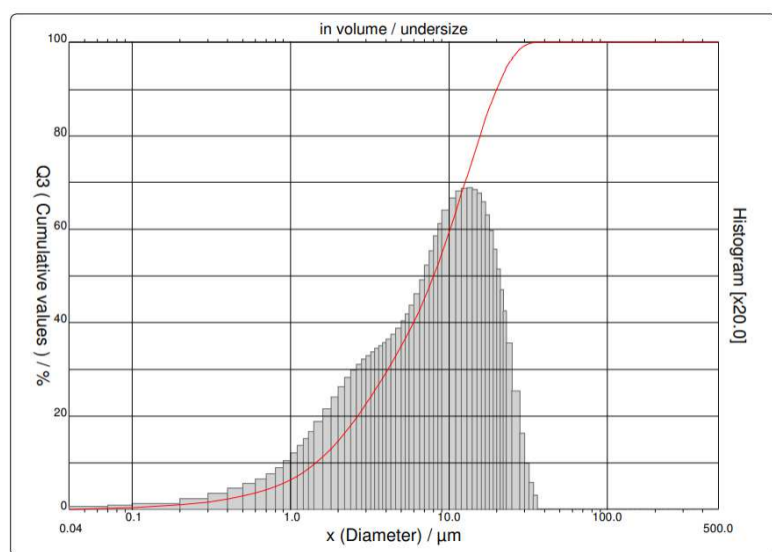
167 The wind tunnel has a particle generator that is made up of a compressed air duct, dust reservoir
168 with injector, and a concentration regulation valve installed at its inlet which dispenses dry coal
169 dust into the wind tunnel. The injected coal dust goes through an aerosol dispersion system to
170 ensure a homogenous distribution of coal dust particles across the cross section of the wind tunnel.
171 The outlet of the wind tunnel is connected to a dust collector that also enables exhausting type
172 airflow through the wind tunnel. The fan drives air through the wind tunnel at a velocity of 1.0 m/s
173 which is the normal air velocity in underground mines (Roghanchi et al., 2016). The wind tunnel
174 has a platform built at the monitoring location which is 25.0 cm from the top of the tunnel on
175 which the sensors and the nozzles for the monitors are installed.



176

178 2.3 Calibration procedure

179 The coal dust used for this experiment is the Keystone mineral black 325 with a density of
 180 $1,220 \text{ kg/m}^3$ with particle sizes in the range of $0.04 \mu\text{m}$ to $35.00 \mu\text{m}$. Detailed characteristics and
 181 particle size distribution of this coal dust can be observed in Figure 3 (A. R. Kumar, 2018). Prior
 182 to the injection of coal dust particles, the two PMS sensors, APS, PDM, two Airtreks, and two
 183 Gaslabs were placed on the monitoring platform in the wind tunnel. The inlets to the sensors and
 184 monitors were placed very closely to one another to minimize spatial differences in particle
 185 concentration in such a way that did not cause interference with each other's exposure to airflow.
 186 Regarding the APS and PDM, the monitors were kept outside the wind tunnel and particles were
 187 sampled from the wind tunnel through nozzles which were positioned to face the flow in the tunnel.
 188 The remaining sensors and monitors were placed inside the wind tunnel with their inlets facing the
 189 flow. It was imperative to ensure that particle concentration at the sampling locations stayed within
 190 10% variation which was observed prior to the start of the experiments using the PDM. This was
 191 ensured by performing a preliminary test measuring and comparing the concentrations across the
 192 sampling location within the wind tunnel using the PDM. The uniform concentration maintained
 193 was the precaution used to ensure that variation in dust concentration between the sensors and
 194 monitors was insignificant.



197 MSHA coal dust regulation is based on end-of-shift Time Weighted Average concentrations of
198 1.5 mg/m³ (MSHA, 2014). The dust coal concentration in mines should typically fluctuate around
199 this value, therefore we investigate the sensors' responses to different concentration levels ranging
200 from 0 to 3.0. The coal dust injection rate was adjusted throughout the course of the experiments
201 within that range depending on the test being performed.

202 The clock times on all sensors and monitors were reset to synchronize the time stamps.
203 Although the APS and PMS sensors were programmed to record real time concentrations every
204 15.0 seconds, the Airtrek monitor reported concentrations every 30.0 seconds, while the Gaslab
205 reports concentrations every 2.0 seconds. For these sensors and monitor that record their outputs
206 multiple times within a minute, their readings were averaged to get minute-by-minute
207 concentrations for all the sensors to be comparable with the PDM. This data is then used in the
208 evaluation and calibration procedure. The PDM's reported time weighted average (TWA)
209 concentration data were converted to minute-by-minute real-time concentrations using Equation 1
210 to be consistent with all the other sensors' data. In this equation, TWAn is the time weighted
211 average at each time step, C_n is the real time concentration measured, T is the time interval between
212 successive measurement and Tn is the total number minutes at time n.

$$C = \frac{TWAn \times Tn}{T} - (C_1 + C_2 + C_3 \dots C_{n-1}) \quad \text{Equation 1}$$

213

214 2.4 Calibration matrices

215 Low-cost PM monitors were evaluated and calibrated based on five calibration matrices:
216 accuracy (linearity), precision, lower limit of detection, upper limit, and temperature and relative
217 humidity influences. These matrices were adopted from the low-cost PM sensor evaluation
218 protocol proposed and used by United States Environmental Protection Agency (US-EPA) (US-
219 EPA, 2013; Williams et al., 2014) the US Air quality sensor performance evaluation center (AQ-220
SPEC) (Papapostolou et al., 2017; Polidori et al., 2017) and European Metrology Research 221
Program (EURAMET) (Spinelle et al., 2013) which have proven to be comprehensive and 222
effective for low-cost PM sensors. These matrices are elaborated in the following sections.

223 2.4.1 Linearity

224 The accuracy of PM sensors is the closeness of sensor measurements to actual concentrations.
225 In the linearity test, sensors and reference monitors were exposed to the same concentrations and
226 environmental conditions within the wind tunnel. During the test, the coal dust injection rate was
227 changed every 10.0 minutes between 0 and 3.0 mg/m³. During this test, concentrations
228 occasionally spiked above the target 3.0 mg/m³ for a few seconds after which valves were quickly
229 readjusted to the correct levels. This, however, allowed us to observe the characteristics of the
230 sensors at peak concentrations beyond 3.0 mg/m³. The linearity of the PMS sensors and the other
231 monitors were assessed using the correlation coefficient from linear regression by plotting the
232 output of monitors against PDM and APS. The concentrations measured by the reference monitors
233 were used as the independent variable, while the concentrations measured by the sensors were
234 reported as dependent variables. Using both the PDM and APS as reference monitors, each sensor
235 is evaluated with both the PDM and APS. The linearity of each sensor and monitor, which is an
236 indication of a monitor's accuracy, is evaluated by the R-squared value calculated using the
237 ordinary least square (OLS) linear regression method. The accuracy of a sensor is lower for those
238 with lower linearity values. The linear regression models generated from this evaluation was then
239 used to derive the calibration equation to improve the accuracy of the PMS to the accuracy of the
240 PDM.

241 2.4.2 Precision

242 The sensors' precision was evaluated by the repeatability of the sensors. This was determined
243 by the dispersion of the sensors' measured values at a constant concentration. This would give us
244 the understanding of the consistency and reliability of the PMS outputs in an extended use. Five
245 concentration levels were used for this test - 0.5 mg/m³, 1.0 mg/m³, 1.5 mg/m³, 2.0 mg/m³ and 3.0
246 mg/m³. At each concentration level, conditions were kept constant in the wind tunnel and
247 measurements were taken with sensors for 60 mins. The spread of a sensor's output was
248 determined by the descriptive statistical parameter of interquartile range in boxplots. This
249 measured the spread of the middle 50 % of the data points from the sensors. The interquartile range
250 (IQR) is calculated using the equation in Equation 2 where IQR is the interquartile range, Q1 is
251 the first quartile and Q3 is the third quartile of the data. Q1 is determined by the ((n+1)/4)th term
252 of the distribution while Q3 is determined by the (3(n+1)/4)th term of the distribution. This was

253 repeated for the two reference monitors as well to compare the trend of spread of the sensors with
254 the reference monitors.

255

$$IQR = Q3 - Q1$$

Equation 2

256 2.4.3 Limit of detection (LOD)

257 LOD describes the lowest concentration limit of sensors that significantly differentiates from
258 sensor outputs at blank concentrations. This tells how the sensors will reliably differentiate
259 concentration changes from instrument noise, which is the short-term deviations in measurements
260 about the mean of a stable concentration which are not caused by changes in concentrations.
261 Different from LOD, the lower limit of sensors was also evaluated as the average sensor output at
262 zero coal dust concentration. The LOD for the low-cost sensors were evaluated by subjecting them
263 to 0.0 mg/m³ coal dust concentrations over a 60-minute period. This blank condition was be
264 generated by filling the chamber with clean air with no particles and completely shutting off the
265 valves to the dust injection system. For this experiment, air is considered clean when the PDM and
266 APS reference monitors measures 0.0 mg/m³. Based on outputs of sensors under these conditions,
267 LOD is calculated using Equation 3 (Kaiser & Specker, 1956) where k is the slope from the fitted
268 linear regression model, and σ_{blk} is the standard deviation. In this experiment, these parameters
269 were calculated based on the 60 measurements taken over a testing period of 1 hour.

270

$$LOD = \frac{3\sigma_{blk}}{k}$$

Equation 3

271

272 2.4.4 Upper concentration limits

273 The upper concentration limit is the concentration at which a 10 unit increase in reference
274 monitors' measurements is unproportionally characterized by a 0.2 unit or an exponential increase
275 in the outputs of low-cost sensors. This concentration serves as the maximum concentration that a
276 sensor is capable of measuring with an acceptable degree of accuracy. Upper limits vary

277 significantly among the various low-cost PM sensors. Even though manufacturers report certain
278 values as the upper limits, usually 1.0 mg/m^3 , it is important to evaluate the upper limit to
279 determine if these limits differ for coal dust particles. The results from the linearity test described
280 in section 2.4.1 was analyzed to determine the operational range for the sensors and to determine
281 the upper limits for each sensor. The inflection point of their response curves (also known as the
282 knee of the curve) was determined as a sensor's upper limit using Equation 4. The maximum k
283 value on the curve determines the inflection point at which the linearity of the sensor ends.

$$k(x) = \frac{|f''(x)|}{[1 + (f'(x))^2]^{3/2}} \quad \text{Equation 4}$$

284

285 2.4.5 Influence of temperature and relative humidity

286 A 2^2 factorial design was used to determine if the temperature and relative humidity changes
287 have a significant impact on dust monitors' readings at low and high coal dust concentration levels.
288 The temperature and relative humidity factors each had two levels, high (+) and low (-). For these
289 tests, low temperatures ranged from 20 to 24°C whereas high temperatures ranged from 26 to 40°C
290 which represents typical underground conditions as the temperature in most mines range from 15
291 and 35°C . Low RH ranged from 20 to 30% while high RH ranged from 35 to 45%. Even though
292 RH in mines can exceed 45%, the challenge of simulating higher RH in the lab limited testing at
293 higher RH values. At each concentration level, four tests were performed at different levels of
294 temperature and relative humidity as shown in Table 1. The order of tests was randomized within
295 each concentration. Each test lasted for 60 minutes. with at least of 5 minutes. stabilization time
296 between tests when the conditions are changed. All 0.5 mg/m^3 concentration tests were performed
297 on 4/18/2022, and the 1.5 mg/m^3 concentration tests were performed on 4/19/2022. A 2 factorial
298 ANOVA analysis of variance was used to evaluate the effect of temperature and relative humidity
299 on the performance of the low-cost PM sensors.

300 The low temperature and relative humidity conditions were achieved using the lab ambient
301 temperature and humidity regulated by the building HVAC system. The high temperature and
302 humidity were achieved by operating a Honeywell heater and a Honeywell cool moisture

303 humidifier, which are displayed in Figure 4 installed at the inlet of the wind tunnel.



304

305 *Figure 4. (a) the Honeywell turbo force power heater and (b) the Honeywell infrared cool moisture humidifier*

306 *Table 1. Experimental design for 0.5 and 15 mg/mg concentration at different temperature and humidity levels*

Test Name	Temperature	Humidity
TLHL0.5	-	-
THHL0.5	+	-
TLHH0.5	-	+
THHH0.5	+	+
TLHL1.5	-	-
THHL1.5	+	-
TLHH1.5	-	+
THHH1.5	+	+

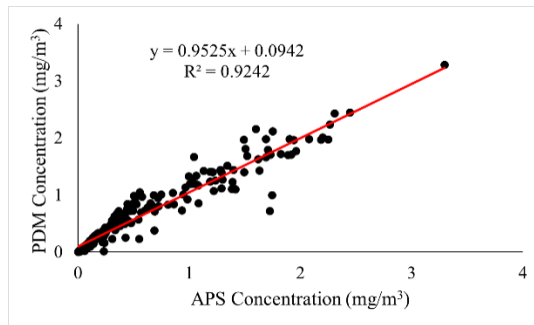
307

308 3 Results

309 3.1 Linearity

310 Prior to the evaluation of the sensors, the two reference monitors were compared beforehand
311 to determine their accuracy of and to determine if any reference monitors had any errors which
312 would eventually affect the sensors' calibration models. Figure 5 shows the correlation obtained
313 from comparing the respirable particle size concentrations from the PDM with the APS. The PDM
314 uses the BGI HD cyclone with precise D₅₀ cut off point of 4.37 μm which has a proven significantly

315 low bias relative to the International Standards Organization (ISO) respirable size selection curve.
316 Since it is practically impossible for the APS to emulate the performance and behavior of the
317 theoretical respirable particle size selection curve, the concentration of particles within the 4.37
318 μm size bin is used in this analysis (Belle, 2017) . When the data from PDM and APS were
319 compared, a remarkably high linearity was observed between them. The R-squared value of 0.92
320 indicates a high correlation between them. In PM monitoring studies, an R-squared above 0.80 is
321 generally considered as highly correlated, with R-squared values from 0.60 to 0.80 representing
322 moderately correlated monitors, while a measure of R-squared below 0.60 is considered to have
323 low correlation (Kelly et al., 2017; Sayahi et al., 2019). A statistical test performed on these results
324 gave a P-value of 0.00 indicating strong statistical significance of these results. It is apparent that
325 despite the two monitors operating on different PM measurement principles, the difference in
326 technologies had no significant impact on their correlation. Both monitors were seen to be highly
327 accurate and appear to be equally responsive to coal dust particles. This explains why both
328 monitors are recognized for their high accuracies. As much as the APS is not recognized as a coal
329 dust monitor, it has shown a high level of accuracy to be used as reference monitor for coal dust
330 monitoring.



331

332 *Figure 5. Correlation between PDM reference monitor and the APS reference monitor*

333 To calibrate the low-cost PM sensors, we evaluated the linearity of each sensor by analyzing
334 the relationship of the output of the PDM and APS against each sensor. Figure 6 displays the
335 statistical plots for the pairwise correlation between the sensors and reference monitors. Prior to
336 the evaluation, the boxplot algorithm for outlier detection was used to filter out data points which
337 were flagged as outliers. The PMS low-cost PM sensors had the best linear correlation among all
338 the sensors under evaluation while the Airtreks and Gaslab monitors had progressively lower
339 performance, respectively.

340 As can be seen from the plots, a considerably high linearity was recorded for both PMS sensors
341 against both reference monitors. High R-squared values of 0.88 and 0.90 was recorded for PMS1
342 and PMS2 respectively with the PDM at P values of 0.00 for both sensors. These results agree with
343 several previous studies which have obtained similar high linearity values for the PMS sensors
344 (Sayahi et al., 2019; Y. Wang et al., 2015) . However, relatively lower R-squared values were
345 observed for the same sensors using the APS as reference monitor with R-squared values of 0.70
346 and 0.73 for PMS1 and PMS2 respectively. P-values generated for this statistical analysis were
347 0.01 and 0.02 for PMS1 and PMS2 respectively highlighting the statistical significance of the
348 outputs. It should be noted that these results are only true for testing concentrations below 3.0
349 mg/m³. While other studies have recorded relatively higher R-squared values for the same sensors,
350 this was only achieved when NaCl or Arizona road dust are used for the testing. Coal dust on the
351 other hand, has particle characteristics which are different from these particles and so the sensors
352 could react to them.

353 The intra-model correlation between the two PMS sensors was found to be 0.97 with a P-value
354 of 0.00 which makes them exceptionally agreeable with each other and can be calibrated using the
355 same calibration model. The PMS can confidently measure coal dust concentrations provided the
356 concentrations stay below 3.0 mg/m³.

357 Although these results point to an acceptable level of accuracy for the PMS sensors, a striking
358 characteristic was observed during the test when concentrations went above 3.0 mg/m³. Beyond
359 this concentration, the PMS sensors reported excessively high outputs which were unrealistic and
360 disproportional with the actual concentration level. For example, the sensor concentrations reached
361 as high as 60.0 mg/m³ when concentration levels within the wind tunnel was below 5.0 mg/m³ as
362 indicated by the APS. These data points, as well as all other outliers for the other sensors' data
363 were therefore eliminated from the statistical analysis as outliers using boxplot algorithms as
364 keeping them on the plots would make the plots unreadable. This characteristic of the PMS sensors
365 has not been observed in previous studies due to generally low testing concentrations used. In
366 those studies, PMS testing concentrations ranged between 0 and 1 mg/m³.

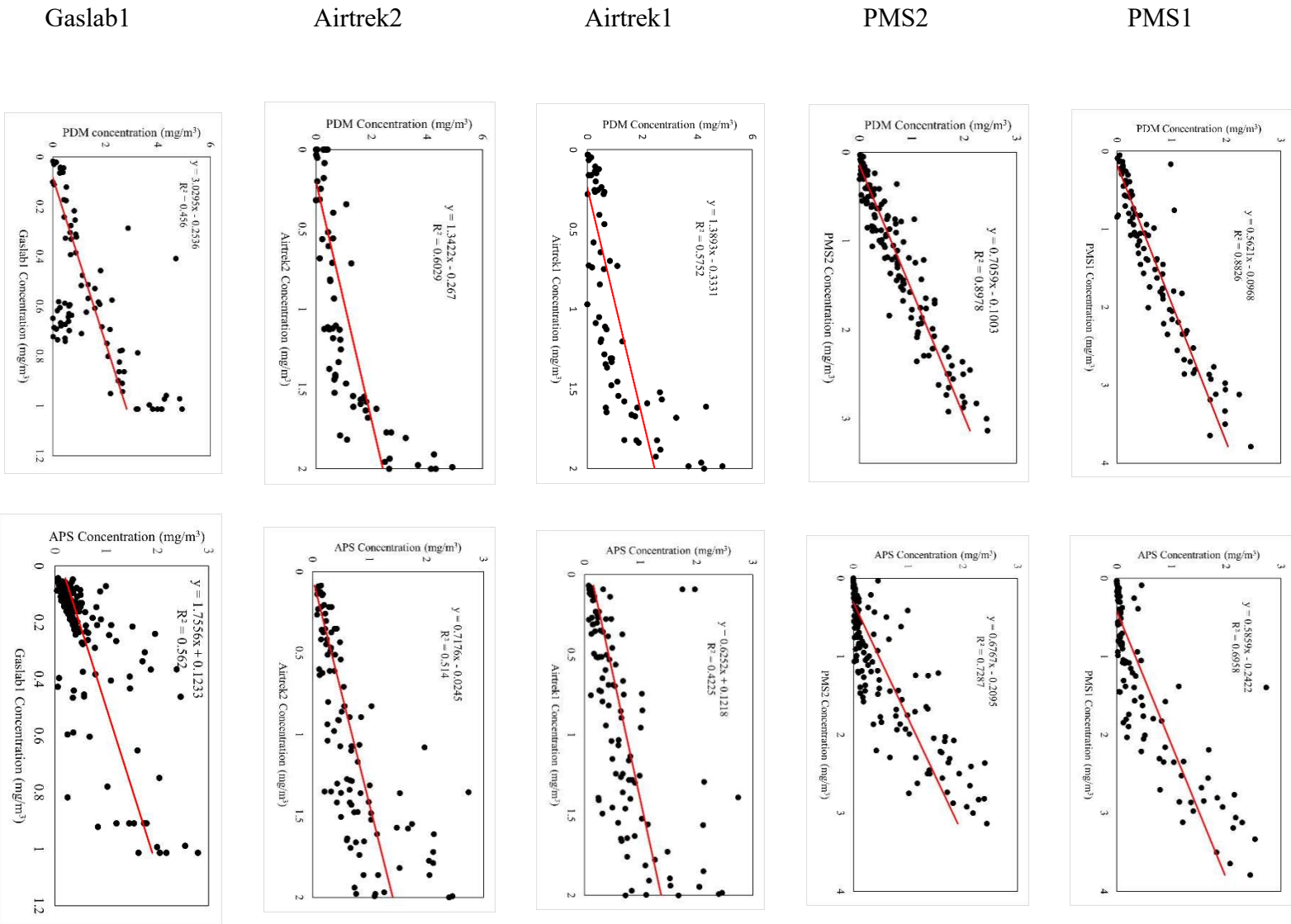
367 Airtrek sensors had slightly lower linearity values as compared with the PMS sensors. As can
368 be seen from the plots displayed in Figure 6, at concentrations below 2.0 mg/m³ when the Airtrek

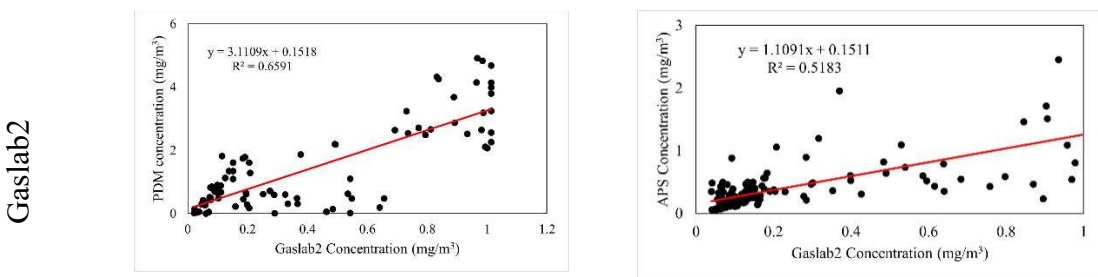
369 sensors reported 1.5 mg/m³, both Airtrek 1 and Airtrek 2 appeared to have a higher linear
370 correlation with the reference monitors. This fairly agrees with manufacturer's datasheet stating
371 that the Airtrek has a measurement range of up to 1.0 mg/m³ even though it can report
372 concentrations to 2.0 mg/m³. However, when concentrations within the wind tunnel exceeded 2.0
373 mg/m³ when the Airtrek sensors reported 1.5 mg/m³, their outputs began to steeply approach 2.0
374 mg/m³ giving the overall Airtrek response an exponential look. This was because the Airtrek
375 sensors would still report concentrations beyond 1.5 mg/m³ but with less accuracy, and report 2.0
376 mg/m³ for all concentrations which are sensed by the sensors to be beyond 2.0 mg/m³. A linear
377 regression statistical analysis to determine the accuracy of the The Airtreks resulted in R-squared
378 values of 0.58 and 0.60 for Airtrek1 and Airtrek2 respectively using the PDM as reference monitor.
379 P-values generated from the statistical analysis were both 0.00 against the PDM emphasizing on
380 its statistical significance. It was also found that Airtrek1 and Airtrek2 had R-squared values of
381 0.42 and 0.51 respectively using the APS as reference and P-values of 0.00 for each sensor. It can
382 be seen from these results that these sensors can be reliable for concentrations below 1.0 mg/m³.
383 Between these sensors, there is an apparent high intra-model linearity with an R-squared of 0.73
384 with a P-value of 0.01. With a robust calibration model, individual calibration models are not
385 required since a single calibration model can fit these sensors to achieve improved performance.

386 The Gaslab sensors had the lowest linearity among the three sensor models under evaluation.
387 Gaslab1 reported R-squared values of 0.46 and 0.56 for PDM and APS respectively with P-values
388 0.00 each, whereas Gaslab2 reported linearity values of 0.66 and 0.52 for PDM and APS
389 respectively with P-values of 0.00. The two Gaslab sensors recorded the lowest intra-model
390 correlation of 0.23 among all the sensors while generating a P-value of 0.02. Much of the non-391
linearity between these sensors and the reference monitors was due to the limited range of the 392
gaslab sensors which makes them report their maximum limit of 1.0 mg/m³ even when the 393
concentration exceeded that. As seen in Figure 6, it can be observed that these sensors reported no 394
output beyond 1.0 mg/m³ even when concentrations within the wind tunnel exceeded 1 mg/m³. 395
These results confirm the specifications of the Gaslab monitors by the manufacturers having a 396
measurement range of 0.0 to 1.0 mg/m³. These sensors may provide reliable monitoring 397
information for environments with lower PM concentrations like indoor offices and home spaces.

PDM

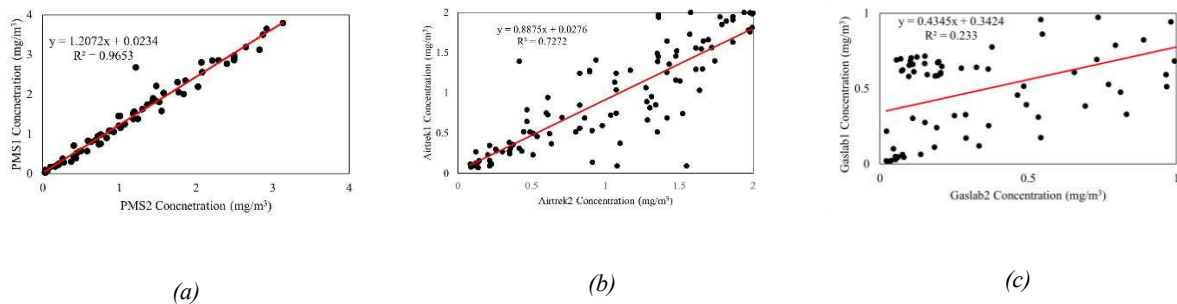
APS





398
399

Figure 6. Pairwise correlation between the two PMS sensors, two Gaslab sensors and the two Airtrek sensors each against the two reference monitors PDM and APS



400
401
402

Figure 7. Intra-mode correlation between the two models of each sensor type (a) PMS5003 sensors (b) Airtrek sensors (c) Gaslab sensors

403 3.2 Precision

404 The results of the tests for precision are displayed in Figure 9. The boxplots of sensor
405 concentrations are shown against true concentrations measured by the PDM using their raw data
406 from the test without removing any outliers. At a constant concentration, the higher the
407 interquartile range of a sensor's distribution shown in the boxplots, the lower the precision of the
408 sensor. The results of the sensors are compared with that of the reference monitors. It can be seen
409 from the PDM and APS results in Figure 8 that even though the concentrations were not perfectly
410 constant, the true concentration range at each concentration level remained constant, indicating
411 their precision and consistence with changes in concentrations. However, in general, there is an
412 increase in the spread of data as concentrations increase, making these sensors unreliable at higher
413 concentrations. It can be seen from the figure that these sensors begin to show imprecision at
414 concentrations 1.5 mg/m³ and above. The spread of the sensors' data is progressively higher than
415 the spread of the reference monitors' data at elevated concentrations.

416 In the case of the PMS1 and PMS2 sensors, the spread of the measurements at concentrations
417 below 1.5 mg/m^3 was determined by the interquartile range set at 1.1 mg/m^3 and 0.5 mg/m^3
418 respectively. As can be seen from Figure 9, the level of precision for both sensors began to
419 noticeably increase as concentrations increased relative to the results from the two reference
420 monitors. At the highest level of concentration where the precision was the worst, the spread of
421 the sensor concentration had increased considerably to 13.3 mg/m^3 and 17.8 mg/m^3 respectively
422 when the concentration reached 3.0 mg/m^3 . This indicates the PMS sensors' inability to reproduce
423 accurate readings at higher concentrations. Therefore, the PMS sensors could be used for mine
424 coal dust monitoring where concentrations are generally low such as inside operators' cabs and on
425 miners underground as personal monitors. It should be noted, however, that the average
426 concentration of coal dust in underground coal mines is 0.55 mg/m^3 (Doney et al., 2019). Therefore,
427 the limitation of imprecision at higher concentrations makes them capable of accurately measuring
428 concentrations within an underground mine under normal operations.

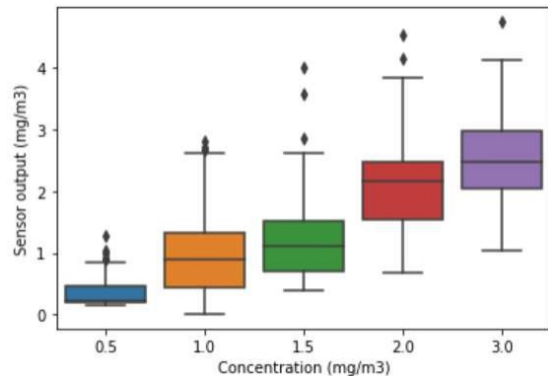
429 Similar to the PMS sensors, the Airtrek sensors showed the highest precision values at
430 concentrations below 1.0 mg/m^3 , which marginally increased while concentrations increased. The
431 spread of concentration outputs for Airtrek1 and Airtrek2 at 0.5 mg/m^3 were 0.38 mg/m^3 and 0.35
432 mg/m^3 respectively which increased progressively to 1.91 mg/m^3 and 1.86 mg/m^3 respectively at
433 3.0 mg/m^3 relative to the reference monitors. A review of the manufacturers' datasheet for the
434 Airtrek sensors reveal that the recommended upper limit for PM monitoring is 1.0 mg/m^3 . Even
435 though the sensors can measure and report concentrations higher than its recommended upper limit,
436 these results indicate that those readings could be imprecise. Deploying these sensors for higher
437 coal dust concentration environment can create misleading results to users.

438 The trend of decreased precision with increasing concentration appeared to be slightly
439 different with the Gaslab sensors. While they showed high precision performance at lower
440 concentrations and lower precision at higher concentrations, their limited upper concentration
441 limits of 2.0 mg/m^3 indicated high precision performances at those concentrations. This was due
442 to the Gaslab sensors consistently reporting 2.0 mg/m^3 when the concentrations went beyond 2.0
443 mg/m^3 . The results from our precision tests confirm that even though these low-cost PM sensors
444 can measure and report concentrations beyond their recommended upper limits, they begin to be
445 imprecise and could report misleading results at higher concentrations. Nevertheless, if the

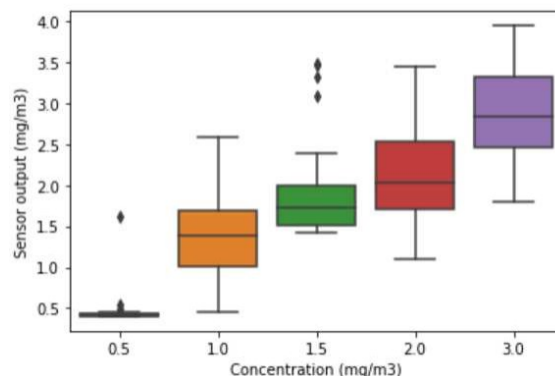
446 imprecise readings from the sensors at higher concentrations appear to be consistent, a more
447 robust calibration algorithm can correct this phenomenon. However, a quantitative number of
448 repetitions of this experiment will have to be performed to determine a consistent trend if one
449 exists.

450 The EPA uses a slightly different method to evaluate sensor precision where the variation
451 about the mean of a sensor output at a constant concentration is determined to be its precision.
452 However, the dynamic testing environment used in this study made it impossible to compare the
453 results to EPA standards which uses a static environment in its testing chamber. Using EPA
454 method of evaluation in this case would result in excessively high variations which would be due
455 to fluctuations in concentrations and not the imprecision of the sensors.

PDM



APS

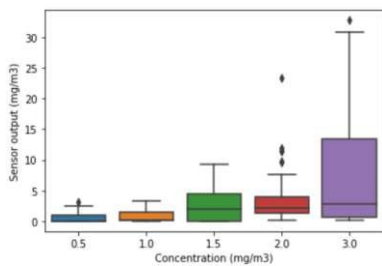


456

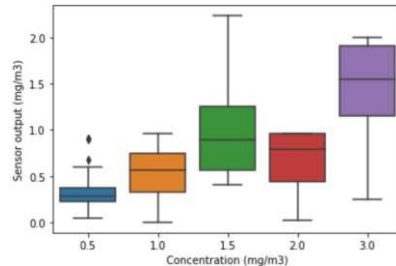
Figure 8. Precision results for reference monitors

457

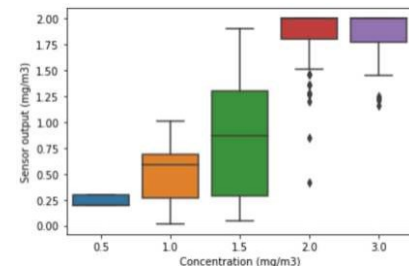
PMS

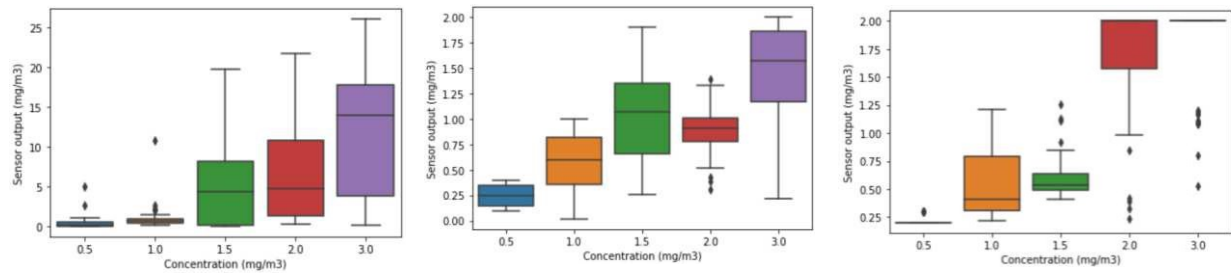


Airtreks



Gaslabs





458

Figure 9. Precision plots for all sensors at concentrations from 0.5 mg/m³ to 3 mg/m³

459

460 3.3 Limit of detection

461 The results from this analysis are presented in Table 2. At 0.0 mg/m³ dust injection
 462 concentration, the PDM recorded 0.00 mg/m³ whereas the APS recorded 0.02 mg/m³. Each of the
 463 PMS sensors recorded an average concentration of 0.01 mg/m³ and LOD values of 0.02 mg/m³
 464 each which was the lowest among the sensors being evaluated. The Airtrek sensors had slightly
 465 higher LOD values where they recorded 0.02 mg/m³ and 0.89 mg/m³ respectively. However, these
 466 Airtrek sensors had the best response to zero concentration giving an average concentration of 0.0
 467 mg/m³. With such accurate outputs at zero concentrations, these sensors would have had a
 468 significantly lower LOD if the linearity test obtained a high linearity for the airtrek sensors. The
 469 Gaslab sensors had the lowest lower limit values with an average concentration of 0.02 mg/m³ at
 470 zero concentration and LOD values of 0.81 mg/m³ and 0.94 mg/m³. It should be noted that due to
 471 the absence of standard calibration curves for these sensors, the calibration curves generated using
 472 linear regression methods in section 3.1 were used for this analysis.

473

Table 2. Lower limits of PMS, Airtrek and Gaslab sensors and their limit of detection

	PMS1	PMS2	Gaslab1	Gaslab2	Airtrek1	Airtrek2
Lower limit (mg/m ³)	0.01	0.01	0.02	0.02	0.00	0.00
LOD (mg/m ³)	0.02	0.02	0.81	0.94	0.02	0.89

474

475 3.4 **Upper concentration limit**

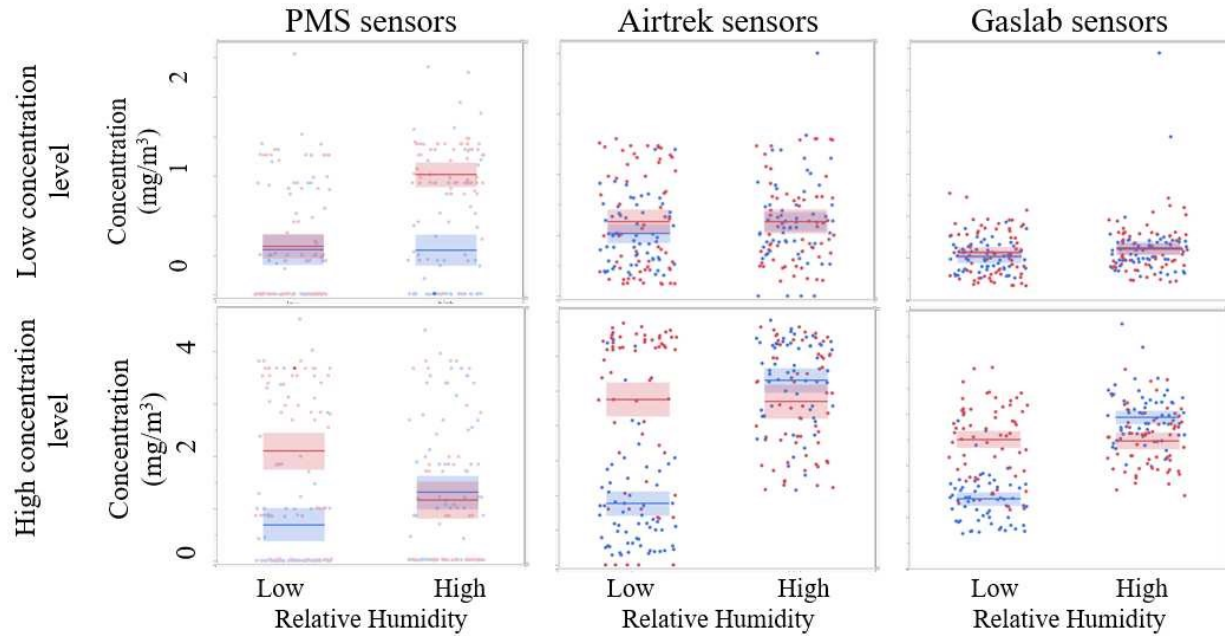
476 In general, the low-cost PM sensors showed significantly lower upper limits as compared with
477 the PDM and APS. This was expected since the APS and PDM are built with more advanced
478 technology to operate in higher concentrations. By plotting the response of the reference monitors
479 against the sensors in section 3.1, the nature of their response were observed and the concentration
480 at which a sensor achieves its maximum value is determined to be the upper limit using Equation
481 4. The results of this analysis are shown in Table 3. The two PMS sensors both demonstrated
482 characteristics of their upper limits at 3.0 mg/m³ of coal dust. Beyond 3 mg/m³, a 10 unit increase
483 in true concentration resulted in a corresponding sensor output of more than 200 % of the true
484 concentration at which point the linearity of the sensor was discontinued. In principle, at higher
485 concentrations when there are many particles within the sensing volume at the same time, these
486 sensors suffer from coincidence errors. The multiple particles present in the sensing volume at the
487 same time are recognized by the sensor as larger and heavier particles in which case the mass is
488 overestimated resulting in such a high concentration compared with the reference monitors.

489 The airtrek sensors showed a slightly lower upper concentration limit of 1.5 mg/m³ and 1.6
490 mg/m³ for Airtrek1 and Airtrek2 respectively. It was observed in the linearity plots of the reference
491 monitors against the Airtrek sensors in section 3.1 that the change in slope from lower
492 concentration to higher concentrations gave the response an exponential curve where the knee of
493 that curve was calculated to be the upper concentration limits. Similar to the Airtrek sensors, the
494 Gaslab sensors were characterized by an exponential curve even though they had a more linear
495 relationship at lower concentrations. The two Gaslab sensors had upper concentration limits of 0.9
496 mg/m³ which was the lowest among the three sensors and close enough to manufacturers specified
497 upper limits. Considering the generally low upper limits of these low-cost PM sensors it is
498 worthwhile to only apply them for lower concentration environments for optimum performances.

499 *Table 3. Upper concentration limits*

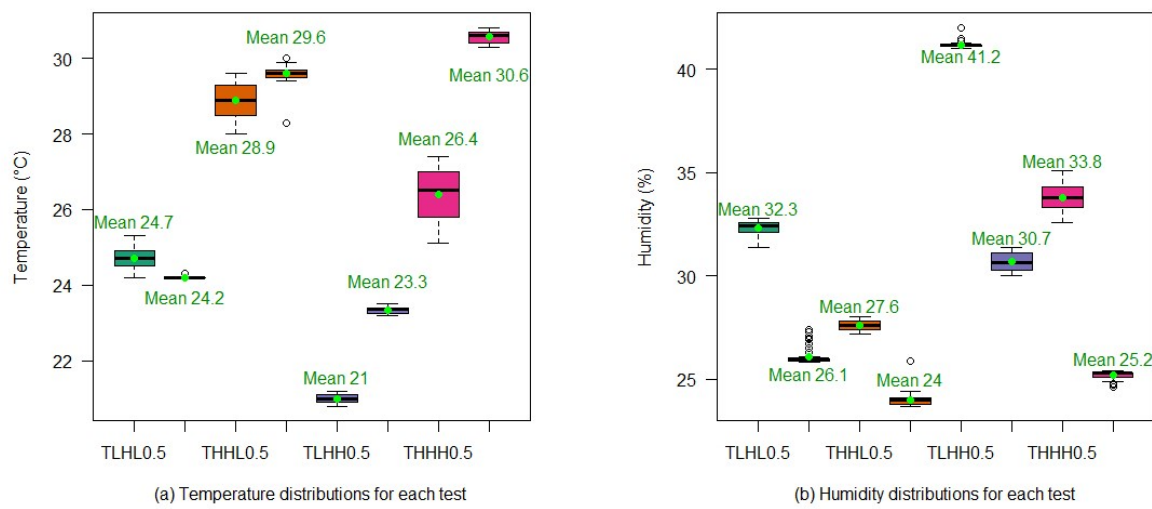
Sensor	PMS1	PMS2	Airtrek1	Airtrek2	Gaslab1	Gaslab2
Upper limit (mg/m ³)	3	3	1.5	1.6	0.9	0.9

501 3.5 Temperature and RH influence



502

503 *Figure 10. Concentrations reported by PMS, Airtrek and Gaslab sensors under different temperature and relative humidity*
 504 *conditions. Results are further elaborated with boxplots.*



505

506 *Figure 11. temperature and relative humidity distribution for the tests*

507 Several studies have found that relative humidity results in a significant bias on the
 508 performance of low-cost PM sensors while others have also suggested no influence. It has been

509 proven that the water droplets in the atmosphere can absorb infrared radiation which is emitted
510 into the measuring cavity of the sensors (Y. Wang et al., 2015). Water vapor can also condense on
511 aerosol particles, causing hygroscopic growth of particles making them seem as though they are
512 larger particles and eventually causing overestimation of particle size and concentrations
513 (Jayaratne et al., 2018). The influence of relative humidity on low-cost PM sensors is highly
514 dependent on the surface properties and composition of the particles. This is the reason why many
515 studies have found a significant influence of relative humidity on these sensors while many others
516 have found little to no influence at all. In this study, both temperature and RH conditions had no
517 significant effect on the performance of the low-cost PM sensors based on the 2k factorial ANOVA
518 analysis of variance. The results of the temperature and RH conditions measured in the wind tunnel
519 is displayed in Figure 11. The temperature achieved within the wind tunnel ranged from 20 degrees
520 Celsius to 31 degrees Celsius while RH was measured to be from 24 % to 44 %. While a wider
521 range of temperature and RH conditions was targeted, it was challenging controlling and
522 maintaining these conditions within the wind tunnel throughout the experiments. Therefore, the
523 results from this test are only valid for the temperature and RH range obtained in this test.

524 Using the ANOVA analysis, all sensors under all conditions of temperature and RH generated
525 F ratios of more than 5.0 % in their respective models. This indicated no significant impact of
526 temperature an RH on the sensors under these temperature and RH factor changes as shown in
527 Figure 11. However, a more in-depth statistical analysis revealed that RH had marginal impact on
528 the performance of the sensors as can be seen from Figure 10. Figure 10 shows boxplots integrated
529 with dot plots of concentrations plotted against relative humidity while overlaying temperature
530 conditions. Red plots represent elevated temperature and blue plots represent low temperature.
531 These results suggest that high RH marginally overestimated the outputs of the Airtrek and Gaslab
532 sensors at higher concentrations of 1.5 mg/m³ especially at lower temperatures. However, this
533 effect was not substantial enough to attribute it to the changes in RH conditions. Other factors such
534 as a concentration fluctuation within the tunnel cause this phenomenon. If RH had significant
535 impact on these sensors, a more robust calibration model would be applied to comprehensively
536 calibrate the sensors to account for the influence of RH on the sensors. To fully understand why
537 RH had no influence on these sensors measuring coal dust, further research is needed to study the
538 surface properties and composition of coal dust particles in detail to substantiate why coal particles
539 are unaffected by atmospheric RH.

540 Temperature, on the other hand, had no impact on the performance on the PMS, Airtrek and
541 Gaslab sensors. Figure 10 shows that there was influence of the temperature rise and fall had on
542 the sensor outputs. These results are consistent with several studies, many of which have
543 established that there is no theoretical dependency of the light scattering principle on temperature.
544 However, some low-cost PM sensors are affected by temperature due to the use of thermal resistors
545 in their operation. In that case, the temperature difference between the outside environment and
546 the thermal resistor could affect the intake flowrate and sensor outputs. In this study, none of the
547 sensors evaluated have that technology. The reference monitors had no impact from the
548 temperature changes since they have temperature and RH control technology in-built. It should be
549 noted that the challenge of difficulty in controlling and maintaining temperature and RH conditions
550 within the wind tunnel could have impacted the findings of this study.

551 **4 Conclusion**

552 Accurate personal monitoring is essential to detect overexposures of the miners working
553 underground in coal mines. This is also critical for recommendations of suitable controls. However,
554 the high cost and size limitations of the PDM limits its usage to only a few miners risking most
555 miners to unknown overexposures. Low-cost PM sensors can measure personal exposure levels
556 for all miners in real time due to their low cost, small size, and light weight. Prior studies have
557 established the potentials for low-cost PM sensors to be used as PM monitors. However, their
558 application for mining-induced PM and underground conditions remained unexplored. Therefore,
559 this study developed a coal dust monitor using the Plantower PMS5003 sensors, evaluated their
560 performance in laboratory experiments together with Airtrek and Gaslab sensors, and calibrated
561 them using linear regression calibration algorithms.

562 It was found that all three sensors under evaluation had different degrees of linearity with the
563 APS and PDM. The PMS sensors had the best linearity with both PDM and APS among all the
564 other sensors under evaluation, with R^2 values ranging from 0.70 to 0.90 and an excellent intra-565
model linearity of 0.97 for concentrations levels below 3.0 mg/m^3 . The Airtrek sensors had slightly 566
lower linearity between 0.0 and 2.0 mg/m^3 , but had lost its linearity at concentration beyond 2.0 mg/m^3 567
giving them an exponential response with the reference monitors. The Gaslab sensors had 568
the least linearity among the sensors with R^2 values ranging from 0.40 to 0.52. All three sensors 569
had precision levels identical to that of the reference monitors at concentration levels below 1.5

570 mg/m³. It was found that beyond 1.5 mg/m³, the sensors experienced a decrease in precision with
571 increasing concentration. PMS sensors demonstrated the highest measurement range with the
572 lowest lower limit of 0.0 mg/m³ and highest upper limits of 3.0 mg/m³. Airtreks generated a closer
573 range of 2.0 mg/m³ while the gaslabs had a range of 1.0 mg/m³. Statistical tests gave P-values of
574 less than 0.05 for all linearity results indicating that these results are reliable beyond the testing
575 results. At concentrations above these limits, the sensors all show challenges reading those
576 concentrations which would potentially give misleading outputs. However, since the upper limit
577 for the PMS sensors are above the PEL for coal dust, the wearer would already be notified. It was
578 also observed that temperature and relative humidity had no significant influence on the
579 performance of these sensors even though an observation of the results show minimal
580 overestimation of sensors' performance at higher RH. The concentration change, however, was not
581 significant enough to attribute it to RH changes.

582 These results provide compelling evidence that the PMS5003 low-cost PM sensor has the
583 potential to monitor coal dust concentrations up to 3.0 mg/m³. Underground coal miners could
584 widely wear this to ensure early overexposure detection and timely control to protect the health of
585 miners. This will eliminate the high expenditure incurred by mines and the federal government
586 associated with treatment of CWP, as well as compensations. This technology is also expected to
587 facilitate improved underground structure and ventilation designs and provide high quality "big
588 data" to facilitates the health studies related to respiratory diseases caused by PM. However, it will
589 be worthwhile to note some limitations that still need to be investigated. During the tests, the
590 research team had the limitation of achieving RH conditions higher than 45%. While RH
591 conditions in underground mines could reach as high as 70%, future studies will need to consider
592 testing at RH of 45% to ~70%. Although the study revealed that the influence of temperature and
593 RH were minimal, these factors should be accounted for in a calibration model in a multiple
594 variable algorithm to make the performance more robust. Future studies should therefore apply
595 models such as multiple linear regression and machine learning algorithms to cover temperature
596 and RH in the calibration models.

597

598

References

600 Badura, M., Batog, P., Drzeniecka-Osiadacz, A., & Modzel, P. (2018). Evaluation of low-cost
601 sensors for ambient PM_{2.5} monitoring. *Journal of Sensors*, 2018.
602 <https://doi.org/10.1155/2018/5096540>

603 Barakeh, Z. Al, Breuil, P., Redon, N., Pijolat, C., Locoge, N., & Viricelle, J. P. (2017).
604 Development of a normalized multi-sensors system for low cost on-line atmospheric pollution
605 detection. *Sensors and Actuators, B: Chemical*, 241, 1235–1243.
606 <https://doi.org/10.1016/j.snb.2016.10.006>

607 Blackley, D. J., Crum, J. B., Halldin, C. N., Storey, E., & Laney, A. S. (2016). Resurgence of
608 progressive massive fibrosis in coal miners — Eastern Kentucky, 2016. *Morbidity and*
609 *Mortality Weekly Report*, 65(49), 1385–1389. <https://doi.org/10.15585/mmwr.mm6549a1>

610 Chen, C. C., Kuo, C. T., Chen, S. Y., Lin, C. H., Chue, J. J., Hsieh, Y. J., Cheng, C. W., Wu, C. M.,
611 & Huang, C. M. (2019). Calibration of Low-Cost Particle Sensors by Using Machine-612
Learning Method. *2018 IEEE Asia Pacific Conference on Circuits and Systems, APCCAS* 613
2018, 111–114. <https://doi.org/10.1109/APCCAS.2018.8605619>

614 De Vito, S., Massera, E., Piga, M., Martinotto, L., & Di Francia, G. (2008). On field calibration of
615 an electronic nose for benzene estimation in an urban pollution monitoring scenario. *Sensors*
616 and *Actuators, B: Chemical*, 129(2), 750–757. <https://doi.org/10.1016/j.snb.2007.09.060>

617 Halterman, A., Sousan, S., & Peters, T. M. (2018). Comparison of respirable mass concentrations
618 measured by a personal dust monitor and a personal DataRAM to gravimetric measurements.
619 *Annals of Work Exposures and Health*, 62(1), 62–71. <https://doi.org/10.1093/annweh/wxx083>

620 Kaiser, H., & Specker, H. (1956). Evaluation and comparison of analytical methods.
621 *Fresenius 'Journal for Analytical Chemistry*, 149(1–2), 46–66.
622 <https://doi.org/10.1007/BF00454145>

623 Kelleher, S., Quinn, C., Miller-Lionberg, D., & Volckens, J. (2018). A low-cost particulate matter
624 (PM_{2.5}) monitor for wildland fire smoke. *Atmospheric Measurement Techniques*, 11(2),
625 1087–1097. <https://doi.org/10.5194/amt-11-1087-2018>

626 Kelly, K. E., Whitaker, J., Petty, A., Widmer, C., Dybwad, A., Sleeth, D., Martin, R., & Butterfield,
627 A. (2017). Ambient and laboratory evaluation of a low-cost particulate matter sensor.
628 *Environmental Pollution*, 221, 491–500. <https://doi.org/10.1016/j.envpol.2016.12.039>

629 Knight, D., Ehrlich, R., Cois, A., Fielding, K., Grant, A. D., & Churchyard, G. (2020). Predictors
630 of silicosis and variation in prevalence across mines among employed gold miners in South
631 Africa. *BMC Public Health*, 20(1), 1–12. <https://doi.org/10.1186/s12889-020-08876-2>

632 Kumar, A. R. (2018). *Dust Control Examination using Computational Fluid Dynamics Modeling
633 and Laboratory Testing of Vortecone and Impingement Screen Filters*. 49.

634 Kumar, P., Morawska, L., Martani, C., Biskos, G., Neophytou, M., Di Sabatino, S., Bell, M.,
635 Norford, L., & Britter, R. (2015). The rise of low-cost sensing for managing air pollution in
636 cities. *Environment International*, 75, 199–205. <https://doi.org/10.1016/j.envint.2014.11.019>

637 Laney, A. S., & Attfield, M. D. (2010). Coal workers' pneumoconiosis and progressive massive
638 fibrosis are increasingly more prevalent among workers in small underground coal mines in
639 the United States. *Occupational and Environmental Medicine*, 67(6), 428–431.
640 <https://doi.org/10.1136/oem.2009.050757>

641 Li, J. (2019). *Recent advances in low-cost particulate matter sensor : calibration and application*.
642 Washington University in St. Louis.

643 Liu, D., Zhang, Q., Jiang, J., & Chen, D. (2017). Performance calibration of low-cost and portable
644 particular matter (PM) sensors. *Journal of Aerosol Science*, 112(May), 1–10.
645 <https://doi.org/10.1016/j.jaerosci.2017.05.011>

646 Liu, H., Tang, Z., Yang, Y., Weng, D., Sun, G., Duan, Z., & Chen, J. (2009). Identification and
647 classification of high risk groups for Coal Workers' Pneumoconiosis using an artificial neural
648 network based on occupational histories: A retrospective cohort study. *BMC Public Health*,
649 9, 1–8. <https://doi.org/10.1186/1471-2458-9-366>

650 Nie, X., Wei, X., Li, X., & Lu, C. (2018). Heat Treatment and Ventilation Optimization in a Deep
651 Mine. *Advances in Civil Engineering*, 2018.

652 Papapostolou, V., Zhang, H., Feenstra, B. J., & Polidori, A. (2017). Development of an
653 environmental chamber for evaluating the performance of low-cost air quality sensors under
654 controlled conditions. *Atmospheric Environment*, 171, 82–90.
655 <https://doi.org/10.1016/j.atmosenv.2017.10.003>

656 Polidori, A., Papapostolou, V., Feenstra, B., & Zhang, H. (2017). *Field Evaluation of Low-Cost*
657 *Air Quality Sensors Field Setup and Testing Protocol. January.* <http://www.aqmd.gov/aq-658>
spec/evaluations/field

659 Pollock, D. E., Potts, J. D., & Joy, G. J. (2009). *Investigation into dust and exposures and mining*
660 *practices in mines in the southern appalachian region.* Society for Mining, Metallurgy, and
661 Exploration, Incorporated, 2009.

662 Sayahi, T., Kaufman, D., Becnel, T., Kaur, K., Butterfield, A. E., Collingwood, S., Zhang, Y.,
663 Gaillardon, P. E., & Kelly, K. E. (2019). Development of a calibration chamber to evaluate
664 the performance of low-cost particulate matter sensors. *Environmental Pollution*, 255.
665 <https://doi.org/10.1016/j.envpol.2019.113131>

666 Sousan, S., Koehler, K., Thomas, G., Park, J. H., Hillman, M., Halterman, A., & Peters, T. M.
667 (2016). Inter-comparison of low-cost sensors for measuring the mass concentration of
668 occupational aerosols. *Aerosol Science and Technology*, 50(5), 462–473.
669 <https://doi.org/10.1080/02786826.2016.1162901>

670 Spinelle, L., Aleixandre, M., & Gerboles, M. (2013). Protocol of evaluation and calibration of low-
671 cost gas sensors for the monitoring of air pollution. In *JRC Technical reports* (Vol. 68).
672 <https://doi.org/10.2788/9916>

673 Systems, E. (2015). *ESP8266EX Datasheet.*

674 Thermo Scientific. (2014). *Model PDM3700* (Issue 42).

675 US-EPA. (2012). List of designated reference and equivalent methods. *Proceedings of the Water*
676 *Environment Federation*, 2005(16), 726–737. <https://doi.org/10.2175/193864705783867675>

677 US-EPA. (2013). *DRAFT Roadmap for Next Generation Air Monitoring. March, 27.*

678 Usman, M., Douglas, A., & Gillies, S. (2015). Real-time monitoring of DPM , airborne Dust and
679 correlating Elemental Carbon measured by two methods in underground mines in USA. *15th*
680 *North American Mine Ventilation Symposium*, 1–7.

681 Volkwein, J. C., Vinson, R. P., Page, S. J., McWilliams, L. J., Joy, G. J., Mischler, S. E., & Tuchman,
682 D. P. (2006). Laboratory and Field Performance of a Continuously Measuring Personal
683 Respirable Dust Monitor. *Usbm Ri 9669*.

684 Wang, D., Zhou, M., Liu, Y., Ma, J., Yang, M., Shi, T., & Chen, W. (2020). Comparison of Risk of
685 Silicosis in Metal Mines and Pottery Factories: A 44-Year Cohort Study. *Chest*, *158*(3), 1050–
686 1059. <https://doi.org/10.1016/j.chest.2020.03.054>

687 Wang, Y., Li, J., Jing, H., Zhang, Q., Jiang, J., & Biswas, P. (2015a). *Labo.* *49*(11), 1063–1077.
688 <https://doi.org/10.1080/02786826.2015.1100710>

689 Wang, Y., Li, J., Jing, H., Zhang, Q., Jiang, J., & Biswas, P. (2015b). Laboratory Evaluation and
690 Calibration of Three Low-Cost Particle Sensors for Particulate Matter Measurement. *Aerosol*
691 *Science and Technology*, *49*(11), 1063–1077.
692 <https://doi.org/10.1080/02786826.2015.1100710>

693 Wang, Y., Li, J., Jing, H., Zhang, Q., Jiang, J., Biswas, P., Wang, Y., Li, J., Jing, H., Zhang, Q.,
694 Jiang, J., & Biswas, P. (2015). *Laborat.* *6826*.
695 <https://doi.org/10.1080/02786826.2015.1100710>

696 Williams, R., Long, R., Beaver, M., Kaufman, A., Zeiger, F., Heimbinder, M., Hang, I., Yap, R.,
697 Acharya, B., Ginwald, B., Kupcho, K., Robinson, S., Zaouak, O., Aubert, B., Hannigan, M.,
698 Piedrahita, R., Masson, N., Moran, B., Rook, M., ... Griswold, W. (2014). *EPA Sensor*
699 *Evaluation Report. May*, *40*. <http://www.epa.gov/research/airscience/docs/sensor-evaluation-report.pdf>
700 http://cfpub.epa.gov/si/si_public_record_report.cfm?dirEntryId=277270

701 Yong, Z., & Haoxin, Z. (2016). *PMS5003 series data manual*.

702

703